submitted to *Geophys. J. Int.*

Magnetic data radial inversion for 3-D source geometry estimation

L.B. Vital[1⋆]

[1] *Observatório Nacional, Gal. José Cristino, 77, São Cristóvão, Rio de Janeiro, 20921-400, Brazil*

Key words: Numerical solutions; Inverse theory; Magnetic anomalies.

⋆ Observatório Ncional, ON

1 METHODOLOGY

1.1 Forward problem

Let $\mathbf{d}^o$ be the observed data vector, whose ith element d_i^o, $i = 1, \ldots, N$, is the total-field anomaly produced by a 3-D source (Fig. 1a) at the point (x_i, y_i, z_i) of a Cartesian coordinate system with x, y and z axes pointing to north, east and down, respectively. We assume that the direction of the total magnetization vector of the source is constant and known. We approximate the volume of the source by a set of L vertically juxtaposed 3-D prisms (Fig. 1b) by following the same approach of Oliveira Jr. et al. (2011) and Oliveira Jr. & Barbosa (2013). The depth to the top of the shallowest prism is defined by z_0 and m_0 is the constant total-magnetization intensity of all prisms. The horizontal cross-section of each prism is described by a polygon with a fixed number V of vertices equally spaced from 0° to 360°, which are described in polar coordinates referred to an internal origin O^k . The radii of the vertices (r_j^k, $j = 1, \ldots, V$, $k = 1, \ldots, L$), the horizontal coordinates (x_0^k and y_0^k, $k = 1, \ldots, L$) of the origins O^k, $k = 1, \ldots, L$, and the depth extent dz of the L vertically stacked prisms (Fig. 1b) are arranged in a $M \times 1$ parameter vector $\mathbf{p}$, $M = L(V + 2) + 1$, given by

$$\mathbf{p} = \left[{\mathbf{r}^1}^\mathsf{T} \quad x_0^1 \quad y_0^1 \quad \ldots \quad {\mathbf{r}^L}^\mathsf{T} \quad x_0^L \quad y_0^L \quad dz \right]^\mathsf{T} , \tag{1}$$

where "$^\mathsf{T}$" denotes transposition and $\mathbf{r}^k$ is a $V \times 1$ vector containing the radii r_j^k of the kth prism. Let $\mathbf{d}(\mathbf{p})$ be the predicted data vector, whose ith element

$$d_i(\mathbf{p}) \equiv \sum_{k=1}^{L} f_i^k(\mathbf{r}^k, x_0^k, y_0^k, dz, z_1^k, m_0), \quad i = 1, \ldots, N , \tag{2}$$

is the total-field anomaly produced by the ensemble of L prisms at the ith observation point (x_i, y_i, z_i). In eq. 2, $f_i^k(\mathbf{r}^k, x_0^k, y_0^k, dz, z_1^k, m_0)$ is the total-field anomaly produced, at the observation point (x_i, y_i, z_i), by the kth prism, with depth to the top $z_1^k = z_0 + (k - 1)dz$. We calculate $d_i(\mathbf{p})$ (eq. 2) by using the Python package Fatiando a Terra (Uieda et al. 2013), which implements the formulas proposed by Plouff (1976).

1.2 Inverse problem formulation

Given a set of tentative values for depth to the top of the shallowest prism z_0 and for the intensity of the total-magnetization of the source m_0, we solve a constrained non-linear problem to estimate the parameter vector $\mathbf{p}$ (eq. 1) by minimizing the objective function

$$\Gamma(\mathbf{p}) = \phi(\mathbf{p}) + \sum_{\ell=1}^{7} \alpha_\ell \, \varphi_\ell(\mathbf{p}) , \tag{3}$$

subject to

$$p_l^{min} < p_l < p_l^{max}, \quad l = 1, \ldots, M \,, \tag{4}$$

where $\varphi(\mathbf{p})$ is the data-misfit function given by

$$\phi(\mathbf{p}) = \frac{1}{N}\|\mathbf{d}^o - \mathbf{d}(\mathbf{p})\|_2^2 \,, \tag{5}$$

which represents the normalized squared Euclidean norm of the difference between the observed data vector $\mathbf{d}^o$ and the predicted data vector $\mathbf{d}(\mathbf{p})$, α_ℓ is a small positive number representing the weight of the ℓth constraint function $\varphi_\ell(\mathbf{p})$ and p_l^{min} and p_l^{max} are, respectively, the lower and upper limits for the lth element p_l of the parameter vector $\mathbf{p}$ (eq. 1). These limits are defined by the interpreter based on both the horizontal extent of the magnetic anomaly and the knowledge about the source. We use the Levenberg–Marquardt method (Aster et al. 2019, p. 240) to minimize the objective function $\Gamma(\mathbf{p})$ (equation 3) and introduce the inequality constraints (equation 4) by using a strategy similar to that presented by Barbosa et al. (1999).

1.3 Constraint functions

We have divided the constraint functions $\varphi_\ell(\mathbf{p})$ (eq. 3), $\ell = 1, \ldots, 7$, used here to obtain stable solutions and introduce a priori information about the magnetic source into three groups.

1.3.1 Smoothness constraints

This group is formed by variations of the first-order Tikhonov regularization (Aster et al. 2019, p. 103) and impose smoothness on the radii r_j^k and the Cartesian coordinates x_0^k and y_0^k of the origin O^k, $j = 1, \ldots, V$, $k = 1, \ldots, L$, defining the horizontal section of each prism (Fig. 1b). They were proposed by Oliveira Jr. et al. (2011) and Oliveira Jr. & Barbosa (2013).

The first constraint of this group is the *Smoothness constraint on the adjacent radii defining the horizontal section of each vertical prism*. This constraint imposes that adjacent radii r_j^k and r_{j+1}^k within each prism must be close to each other. It forces the estimated prism to be approximately cylindrical. We have conveniently rewritten this constraint in matrix form as follows:

$$\varphi_1(\mathbf{p}) = \mathbf{p}^\mathsf{T}\mathbf{R}_1^\mathsf{T}\mathbf{R}_1\mathbf{p} \,, \tag{6}$$

where

$$\mathbf{R}_1 = \begin{bmatrix}\mathbf{S}_1 & \mathbf{0}_{LV\times 1}\end{bmatrix}_{LV\times M} \quad , \tag{7}$$

$$\mathbf{S}_1 = \mathbf{I}_L \otimes \begin{bmatrix}\left(\mathbf{I}_V - \mathbf{D}_V^\mathsf{T}\right) & \mathbf{0}_{V\times 2}\end{bmatrix} \quad , \tag{8}$$

$\mathbf{0}_{LV\times 1}$ is an $LV \times 1$ vector with null elements, $\mathbf{I}_L$ is the identity matrix of order L, "$\otimes$" denotes the

Kronecker product (Horn & Johnson 1991, p. 243), $\mathbf{0}_{V\times 2}$ is a $V \times 2$ matrix with null elements, $\mathbf{I}_V$ is the identity matrix of order V and $\mathbf{D}_V^\mathsf{T}$ is the upshift permutation matrix of order V (Golub & Loan 2013, p. 20).

The second constraint of this group is the *Smoothness constraint on the adjacent radii of the vertically adjacent prisms*, which imposes that adjacent radii r_j^k and r_j^{k+1} within vertically adjacent prisms must be close to each other. This constraint forces the shape of all prisms to be similar to each other and is given by

$$\varphi_2(\mathbf{p}) = \mathbf{p}^\mathsf{T}\mathbf{R}_2^\mathsf{T}\mathbf{R}_2\mathbf{p} \quad , \tag{9}$$

where

$$\mathbf{R}_2 = \Big[\mathbf{S}_2 \quad \mathbf{0}_{(L-1)V\times 1}\Big]_{(L-1)V\times M} \quad , \tag{10}$$

$$\mathbf{S}_2 = \Big(\Big[\mathbf{I}_{L-1} \quad \mathbf{0}_{(L-1)\times 1}\Big] - \Big[\mathbf{0}_{(L-1)\times 1} \quad \mathbf{I}_{L-1}\Big]\Big) \otimes \Big[\mathbf{I}_V \quad \mathbf{0}_{V\times 2}\Big] \quad , \tag{11}$$

$\mathbf{0}_{(L-1)V\times 1}$ is an $(L-1)V \times 1$ vector with null elements, $\mathbf{0}_{(L-1)\times 1}$ is an $(L-1)\times 1$ vector with null elements and $\mathbf{I}_{L-1}$ is the identity matrix of order $L-1$.

The last constraint of this group is the *Smoothness constraint on the horizontal position of the arbitrary origins of the vertically adjacent prisms*. This constraint imposes that the estimated horizontal Cartesian coordinates (x_0^k, y_0^k) and (x_0^{k+1}, y_0^{k+1}) of the origins O^k and O^{k+1} of adjacent prisms must be close to each other. It forces the prisms to be vertically aligned. This constraint is given by

$$\varphi_3(\mathbf{p}) = \mathbf{p}^\mathsf{T}\mathbf{R}_3^\mathsf{T}\mathbf{R}_3\mathbf{p} \quad , \tag{12}$$

where

$$\mathbf{R}_3 = \Big[\mathbf{S}_3 \quad \mathbf{0}_{(L-1)2\times 1}\Big]_{(L-1)2\times M} \quad , \tag{13}$$

$$\mathbf{S}_3 = \Big(\Big[\mathbf{I}_{L-1} \quad \mathbf{0}_{(L-1)\times 1}\Big] - \Big[\mathbf{0}_{(L-1)\times 1} \quad \mathbf{I}_{L-1}\Big]\Big) \otimes \Big[\mathbf{0}_{2\times V} \quad \mathbf{I}_2\Big] \quad , \tag{14}$$

$\mathbf{0}_{(L-1)2\times 1}$ is an $(L-1)2 \times 1$ vector with null elements, $\mathbf{0}_{2\times V}$ is a $2 \times V$ matrix with null elements and $\mathbf{I}_2$ is the identity matrix of order 2.

1.3.2 Equality constraints

PAREI AQUI

This group if formed by two constraints that were proposed by Oliveira Jr. et al. (2011) and Oliveira Jr. & Barbosa (2013) by following the same approach proposed Barbosa et al. (1997) and Barbosa et al. (1999). They introduce a priori information about the shallowest prism and are suitable for outcropping sources.

The *Source's outcrop constraint* imposes that the estimated horizontal cross-section of the shallowest prism must be close to the intersection of the geologic source with the known outcropping boundary. The matrix form of the this constraint is given by

$$\varphi_4(\mathbf{p}) = (\mathbf{R}_4\mathbf{p} - \mathbf{a})^\mathsf{T} (\mathbf{R}_4\mathbf{p} - \mathbf{a}) \,, \tag{15}$$

where $\mathbf{a}$ is a vector containing the parameters defining the polygon that represents the outcropping body

$$\mathbf{a} = \begin{bmatrix} \tilde{r}_1^0 \\ \tilde{r}_2^0 \\ \vdots \\ \tilde{r}_M^0 \\ \tilde{x}_0^0 \\ \tilde{y}_0^0 \end{bmatrix}_{(V+2)\times 1} \,, \tag{16}$$

and

$$\mathbf{R}_4 = \begin{bmatrix} \mathbf{I}_{V+2} & \mathbf{0}_{(V+2)\times(M-V-2)} \end{bmatrix}_{(V+2)\times M} \,, \tag{17}$$

where $\mathbf{I}_{V+2}$ is the identity matrix of order $V+2$ and $\mathbf{0}_{(V+2)\times(M-V-2)}$ is a matrix with null elements.

The *Source's horizontal location constraint* imposes that the estimated horizontal Cartesian coordinates of the origin within the shallowest prism must be as close as possible to a known outcropping point. The matrix form of the this constraint is given by

$$\varphi_5(\mathbf{p}) = (\mathbf{R}_5\mathbf{p} - \mathbf{b})^\mathsf{T} (\mathbf{R}_5\mathbf{p} - \mathbf{b}) \quad , \tag{18}$$

where

$$\mathbf{R}_5 = \begin{bmatrix} \mathbf{B}^\sharp & \hat{\mathbf{0}} \end{bmatrix}_{2\times M} \,, \tag{19}$$

$$\mathbf{B}^\sharp = \begin{bmatrix} 0 & \cdots & 0 & 1 & 0 \\ 0 & \cdots & 0 & 0 & 1 \end{bmatrix}_{2\times(V+2)} \,, \tag{20}$$

and $\mathbf{p}'$ is a vector containing the Cartesian coordinates of the horizontal location of the source given by

$$\mathbf{p}' = \begin{bmatrix} x_0^0 \\ y_0^0 \end{bmatrix}_{2\times 1} \,; \tag{21}$$

1.3.3 Minimum Euclidean norm constraints

Minimum Euclidean norm constraint on the adjacent radii within each vertical prism. This constraint imposes that all estimated radii within each prism must be close to null values. The matrix form of the this constraint is given by

$$\varphi_6(\mathbf{p}) = \mathbf{p}^\top \mathbf{C}^\top \mathbf{C}\mathbf{p}, \tag{22}$$

where

$$\mathbf{C} = \begin{bmatrix} \mathbf{C}^\sharp & \mathbf{0} & \mathbf{0} & \cdots & \mathbf{0} & \mathbf{0} \\ \mathbf{0} & \mathbf{C}^\sharp & \mathbf{0} & \cdots & \mathbf{0} & \mathbf{0} \\ \mathbf{0} & \mathbf{0} & \ddots & & \vdots & \vdots \\ \vdots & \vdots & & \ddots & \vdots & \vdots \\ \mathbf{0} & \mathbf{0} & \cdots & \cdots & \mathbf{C}^\sharp & \mathbf{0} \\ \mathbf{0} & \mathbf{0} & \cdots & \cdots & \mathbf{0} & 0 \end{bmatrix}_{M \times M}, \tag{23}$$

$$\mathbf{C}^\sharp = \begin{bmatrix} 1 & & & & \\ & \ddots & & & \\ & & 1 & & \\ & & & 0 & \\ & & & & 0 \end{bmatrix}_{(V+2)\times(V+2)}; \tag{24}$$

Minimum Euclidean norm constraint on the depth extent of all prisms. This constraint imposes that the estimated depth extent of the prisms must be close to a null value. The matrix form of the this constraint is given by

$$\varphi_7 = \mathbf{p}^\top \mathbf{D}^\top \mathbf{D}\mathbf{p}, \tag{25}$$

where

$$\mathbf{D} = \begin{bmatrix} 0 & \cdots & 0 \\ \vdots & \ddots & \vdots \\ 0 & \cdots & 1 \end{bmatrix}_{M \times M}. \tag{26}$$

ACKNOWLEDGMENTS

REFERENCES

Aster, R. C., Borchers, B., & Thurber, C. H., 2019. *Parameter Estimation and Inverse Problems*, Elsevier, 3rd edn.

Barbosa, V. C. F., Silva, J. B. C., & Medeiros, W. E., 1997. Gravity inversion of basement relief using approximate equality constraints on depths, *Geophysics*, **62**, 1745–1757.

Barbosa, V. C. F., Silva, J. B. C., & Medeiros, W. E., 1999. Gravity inversion of a discontinuous relief stabilized by weighted smoothness constraints on depth, *Geophysics*, **64**(5), 1429–1437.

Golub, G. H. & Loan, C. F. V., 2013. *Matrix Computations (Johns Hopkins Studies in the Mathematical Sciences)*, Johns Hopkins University Press, 4th edn.

Horn, R. A. & Johnson, C. R., 1991. *Topics in Matrix Analysis*, Cambridge University Press, 1st edn.

Oliveira Jr., V. C. & Barbosa, V. C. F., 2013. 3-D radial gravity gradient inversion, *Geophysical Journal International*, **195**(2), 883–902.

Oliveira Jr., V. C., Barbosa, V. C. F., & Silva, J. B. C., 2011. Source geometry estimation using the mass excess criterion to constrain 3-D radial inversion of gravity data, *Geophysical Journal International*, **187**(2), 754–772.

Plouff, D., 1976. Gravity and magnetic fields of polygonal prisms and application to magnetic terrain corrections, *Geophysics*, **41**(4), 727–741.

Uieda, L., Oliveira Jr., V. C., & Barbosa, V. C. F., 2013. Modeling the earth with fatiando a terra, in *Proceedings of the 12th Python in Science Conference*, pp. 96 – 103.

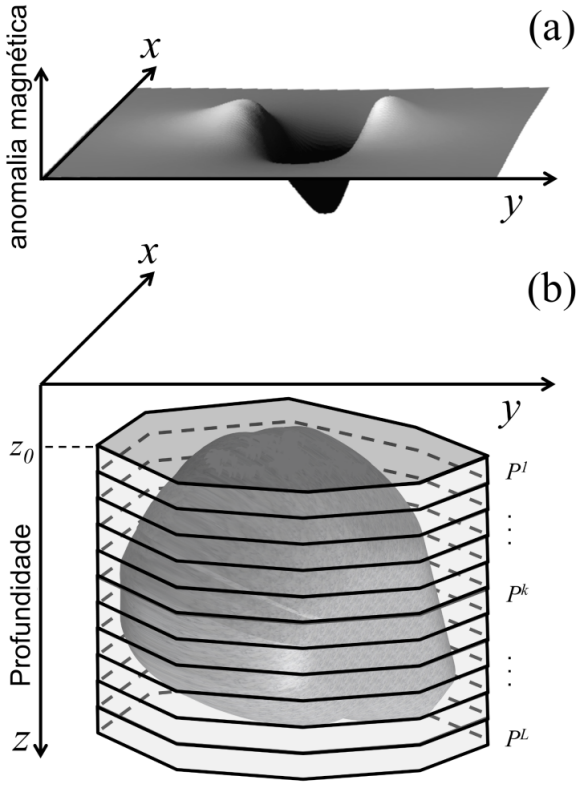

Figure 1. Schematic representation of (a) total-filed anomaly (grey surface) produced by (b) a 3-D anomalous source (dark grey volume). The interpretation model in (b) consists of a set of L vertical, juxtaposed 3-D prisms P^k , $k = 1, \ldots, L$, (light grey prisms) in the vertical direction of a right-handed coordinate system.

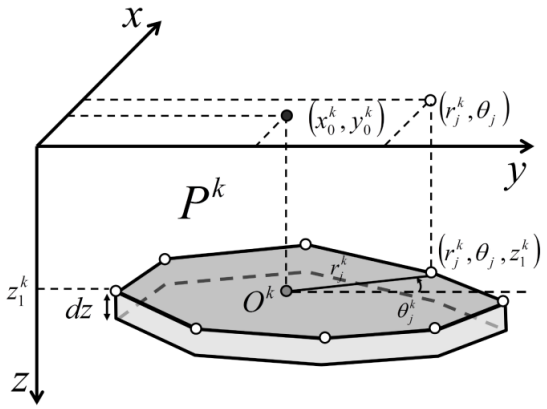

Figure 2. Polygonal cross-section of the kth vertical prism P^k described by V vertices (white dots) with polar coordinates (r_j^k , θ_j^k), $j = 1, \ldots, V$, $k = 1, \ldots, L$, referred to an arbitrary origin O^k (grey dot) with horizontal Cartesian coordinates (x_0^k , y_0^k), $k = 1, \ldots, L$, (black dot).

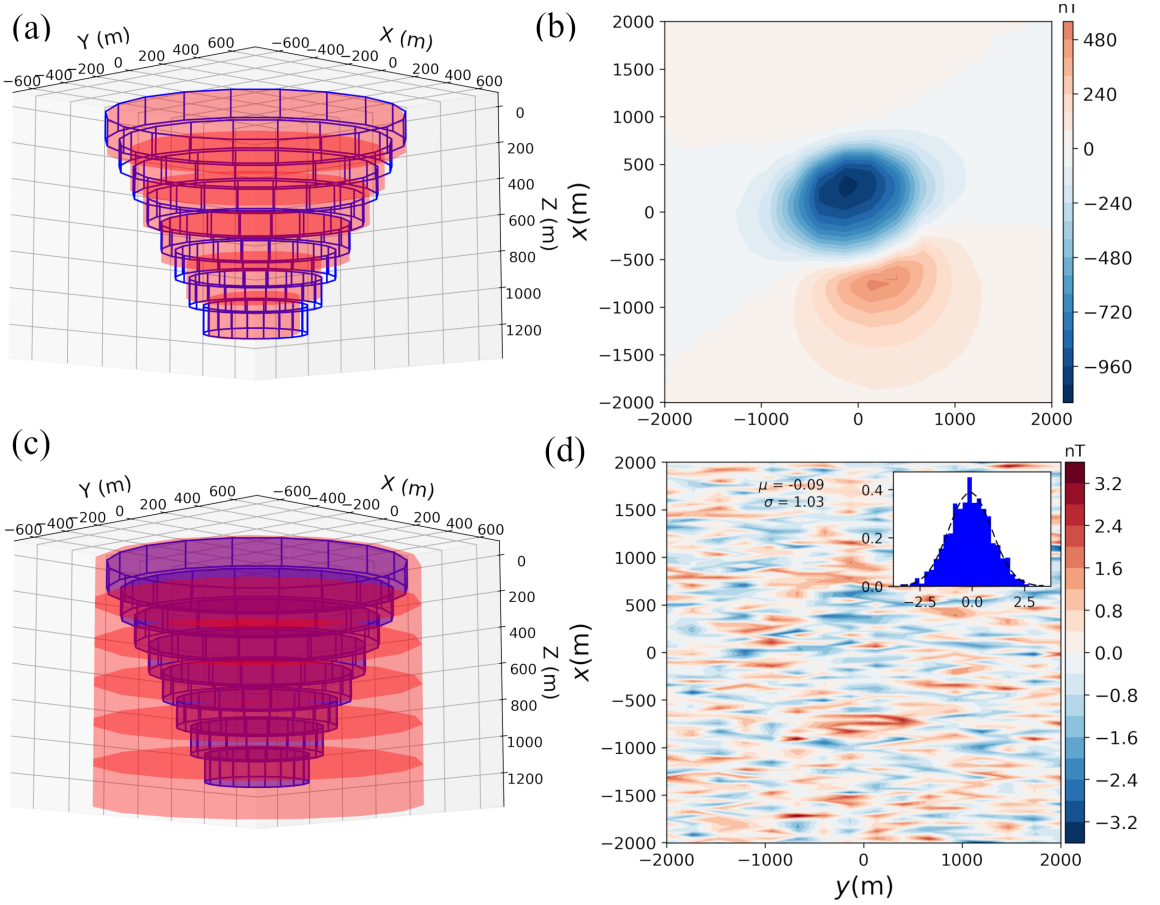

Figure 3. (a) Perspective view of the simple model with the depth to the top $z_0 = 50$ m and the depth extent 1200 m. (b) Synthetic noise-corrupted total-field anomaly produced by the simple model blue prisms in (a). The data was contaminated by a pseudorandom Gaussian noise with mean zero and standard deviation 1 nT. (c) Perspective view of the true (blue lines) and estimated body (red prisms) obtained by inverting the noise-corrupted total-field anomaly in (b). (d) Residuals defined as the difference between the noisy and the predicted (not shown) total-field anomalies; the latter was produced by the estimated body (red prisms in b). The inset in d shows the histogram and the Gaussian curve for the residuals with mean $\mu = 0.1$ nT and standard deviation $\sigma = 5.23$ nT.

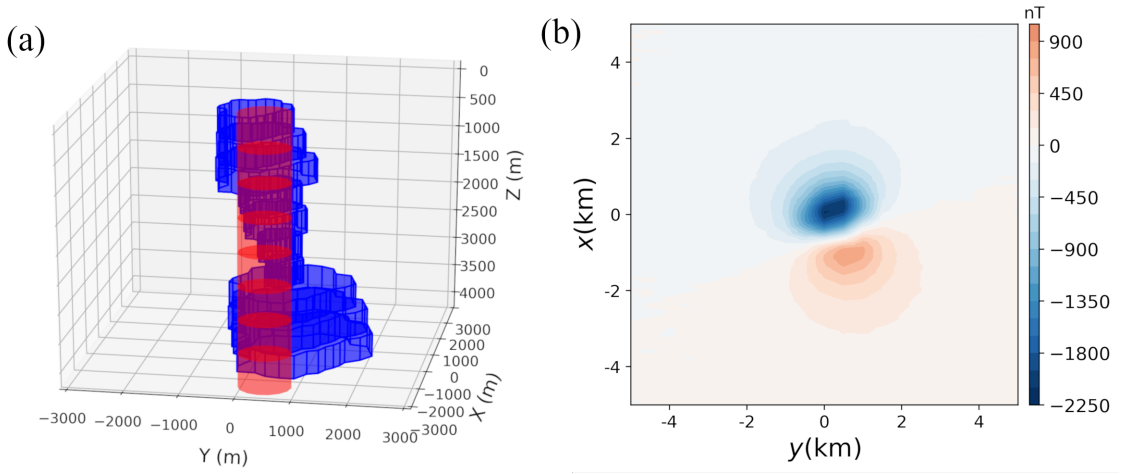

Figure 4. (a) Perspective view of the complex model (blue prisms) with the depth to the top $z_0 = 200$ m and the depth extent 4000 m and the initial guess (red prisms) for the inversion which is a cylinder with radius 500 m and depth extent 4800 m. (b) Synthetic noise-corrupted total-field anomaly produced by the complex model blue prisms in (a). The data was contaminated by a pseudorandom Gaussian noise with mean zero and standard deviation 5 nT.

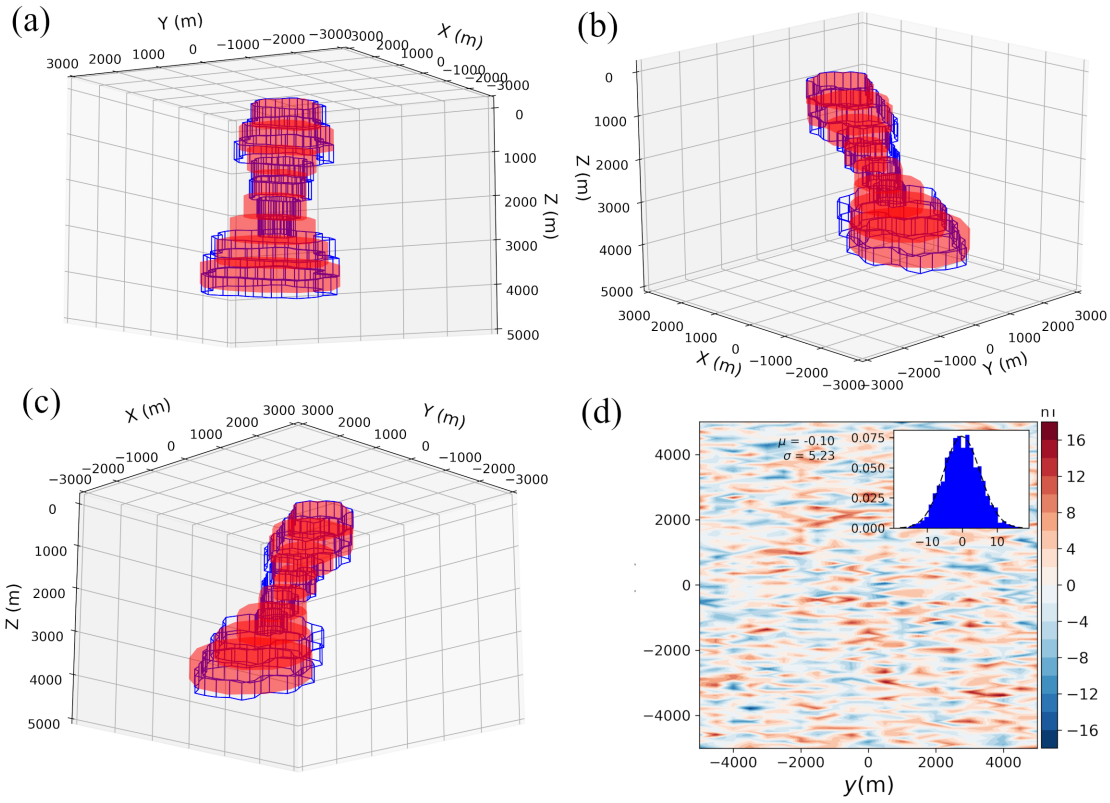

Figure 5. Perspective views of the complex model (blue lines) and the estimate (red prisms) in (a), (b) and (c). (d) Residuals defined as the difference between the noisy and the predicted (not shown) total-field anomalies and the histogram of the residuals (inset in d) with mean $\mu = 0.1$ nT and standard deviation $\sigma = 5.23$ nT. The dashed line on the inset is the Gaussian curve for the residuals.

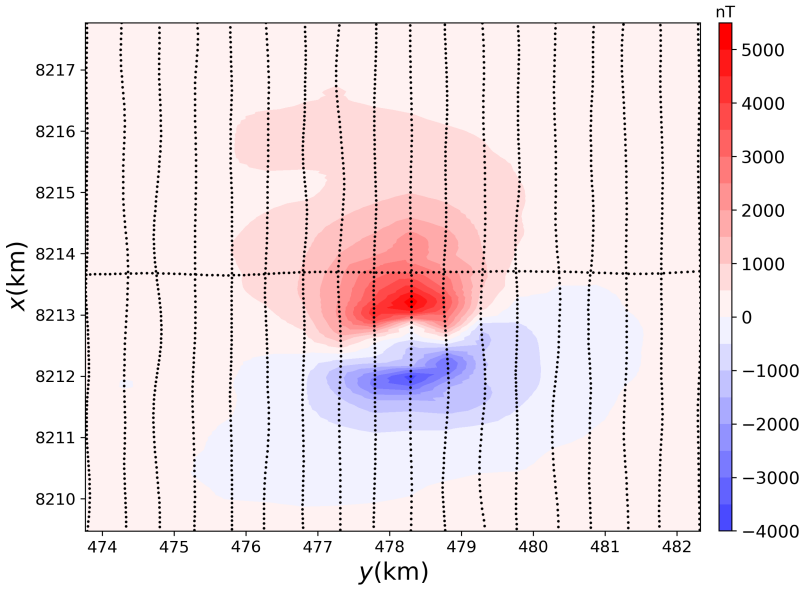

Figure 6. Total-field anomaly of Diorama in GAP. The black dots are the observation points used in this work.

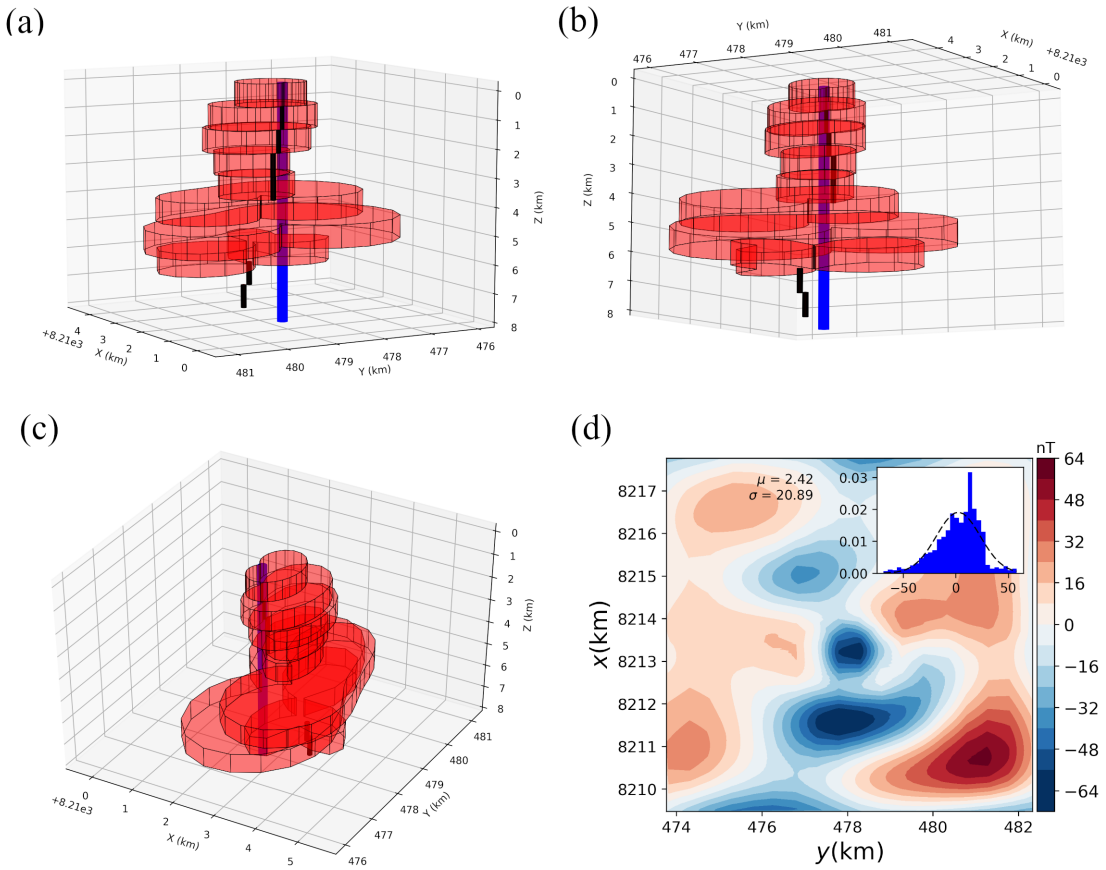

Figure 7. Perspective views of the initial guess (blue cylinder) and the estimated source (red prisms) in (a), (b) and (c). (d) Residuals defined as the difference between the noisy and the predicted (not shown) total-field anomalies and the histogram of the residuals (inset in d) with mean $\mu = 2.42$ nT and standard deviation $\sigma = 20.89$ nT. The dashed line on the inset is the Gaussian curve for the residuals.